Buletin Geoinformasi, Jld.1, No. 2, ms. 71 - 82, September 1997

Gravity Anomaly And Topography Induced By Repeated Fault Motions

Syed Ilias Syed Hashim
Geodesy Section
Directorate of Surveying & Mapping
Kuala Lumpur, Malaysia

Wan Abdul Aziz Wan Mohd. Akib
Centre for Geodetic & Geodynamic Studies
Faculty of Geoinformation Science & Engineering
Universiti Teknologi Malaysia
Skudai, Johor Darul-Takzim

Abstract

The Accumulation Hypothesis deals with the origin of the gravity anomaly and topography around an active fault. This hypothesis was postulated that the gravity anomaly around active faults is the product of repeated fault motions; higher gravity anomaly will occured in compressed areas while lower anomaly in dilated areas. If it is the case, the topography around an active fault can also be interpreted in terms of repeated coseismic elevation change. This paper therefore presents the characters of gravity changes and topography caused by strike-slip faulting at Fujimi Valley, Nagano Prefecture, Japan. In order to compute theoretical gravity changes (Δg) and elevation (h), we use analytical expressions of Δg and Δh caused by faulting on a finite rectangular plane buried in a homogeneoous half-space. The expected gravity anomaly and topography for this test area are compared with the observed data. The analyses have shown that the simple fault model yields gravity anomaly which agrees well with the observations. Similarly, the same model also generates the elevation changes that is consistent with the actual topography of the test area.

1. INTRODUCTION

Peculiar topographical characteristics often appears around active faults. For example, the faulting process built isolated hills and at the same time created sag ponds. A similar phenomenon is occured during the tectonic process at Fujima Valley in Nagano, Japan. This area is bounded by active faults belonging to the Itoigawa-Shizouka Tectonic Line (ITSL). The collision between the Eurasian and North America plates have created peculiar topographical features such as a chain of small isolated hills (tectonic bulges) which are often accompanied by sag ponds nearby, (Nakamura, 1983). On the other hand, theoretical expression of coseismic elevation and gravity changes during an earthquakes are well formulated with the dislocation theory. The dislocation theory can be used to give physical and quantitative explainations not only to gravity anomaly but also to topography around an active fault. Details of the potential and gravity changes caused by point dislocations and by faulting on a finite plane in a semi-infinite medium is given in Okubo, (1992). The expression of point dislocations enable us to evaluate coseismic gravity and elevation changes during a single event and the results can be compared with the actual observations. This paper therefore describes the relationship between gravity anomaly and topography changes with respect the active faults in the test area, Fujimi Valley - Japan.

2. DESCRIPTION OF THE TEST AREA

The town of Fujimi is located in the valley between Mt. Yatsugatake and Akaishi Range, see Figure 1. This area has predominant left-lateral strike-slip on a plane with a high dipping angle. The faults have been active during the late Quaternary and are suspected to have formed several small bulges and sag ponds. However, the fluvial process could have covered it with the debris from the surrounding mountains transported by Takechi river which is running besides the fault line. In the Fujimi Valley, the bulges are extended in longitudinal and transverse direction that can be interpreted as the accumulated result of faulting activities. In this area, the excavation trenching are also clearly identified its precise position of fault traces and the nature of fault.

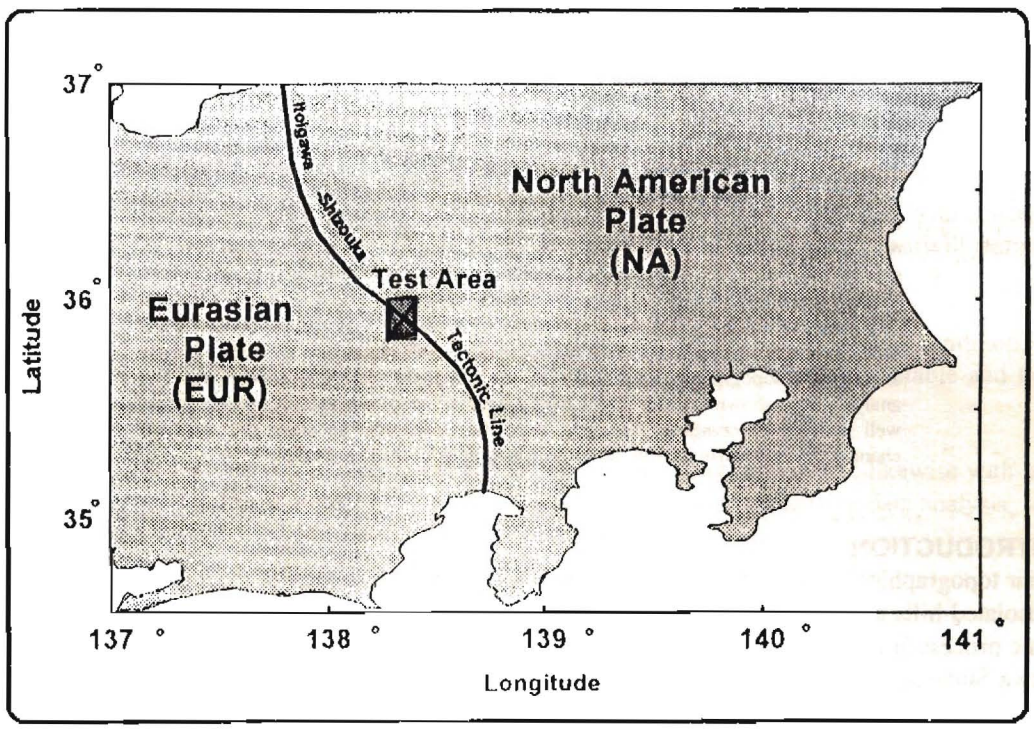

Figure 1 - The Map of Fujimi Valley in Nagano Prefecture, Japan

3. ACCUMULATIVE HYPOTHESIS AND DISLOCATION THEORY

The Accumulative Hypothesis deals with the origin of the gravity anomaly and topography around an active fault. It was postulated that the gravity anomaly around active faults is a product of repeated fault motions, (Okubo et.al., 1990) Also, the topography around the fault areas can be interpreted in terms of repeated coseismic elevation changes (subsidence and uplift). Figure: 2 explains the features of gravity anomaly and topopgraphy caused by strike-slip faulting, i.e. a higher gravity anomaly in the compressed areas while lower gravity anomaly in dilated area. However, characters of gravity changes and topography appeared depends on the slipping or dipping angle of the fault motion.

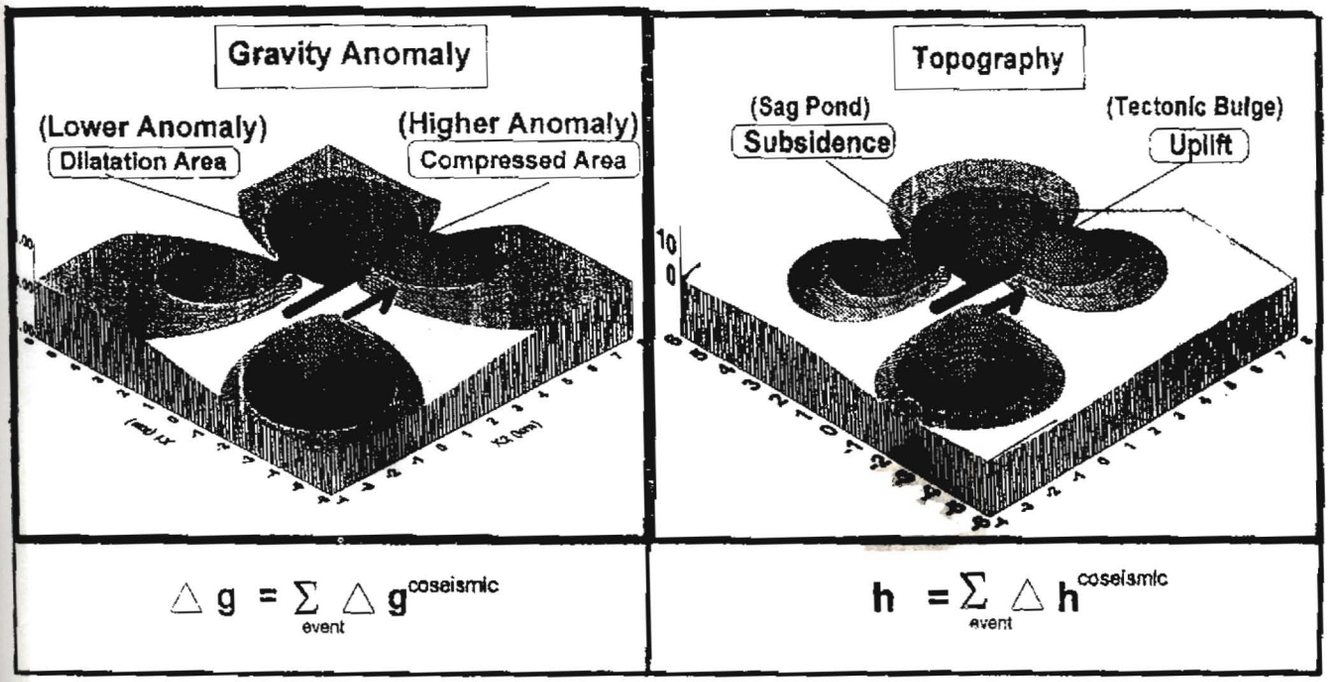

Figure 2 - The Accumulation Hypothesis Related to the Strike-Slip Faulting

The dislocation theory can be used to simulate the observed data. By fitting the calculated gravity anomaly to the observed data, the fault geometry and dislocation vector can be estimated. This is because the model should reflect the gravity changes and the observed topography. The dislocation theory considers deformation due to fault motion on a finite rectangular plane buried in a homogeneous, perfectly elastic half-space. Figure 3 shows the geometry of a fault model in the Cartesian coordinates system where the elastic medium occupies the region of $X_3 < 0$ and X is taken to strike direction of the fault. The fault dimension is represented by length L, width W, depth d, and dip angle δ. The components U_1, U_2 and U_3 denote left-lateral strike slip, thrusting slip and tensile opening, respectively.

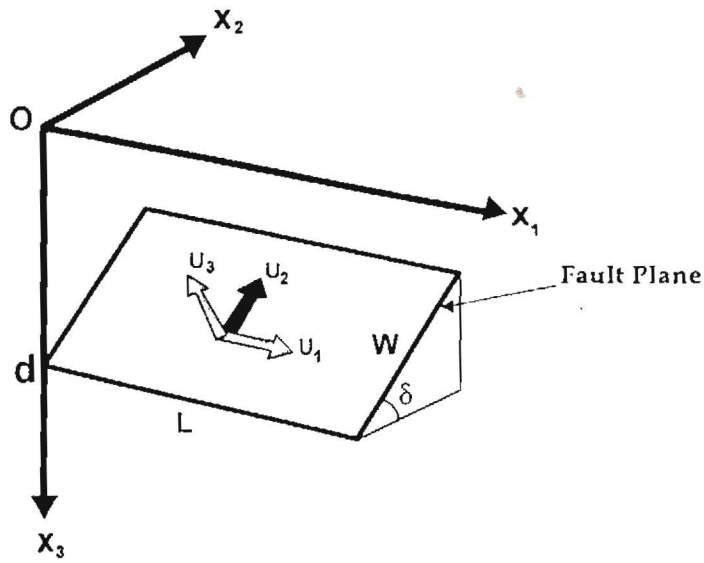

Figure 3 - The Geometry of Faulting on a Finite Rectangular Plane Model

The displacement field u_k for a dislocation on a plane Σ is formulated by Chinnery,(1961) as:

$$u_k = \frac{1}{8\pi\mu}\iint_{\sum}\Delta u_i w_{ij}^k n_j d\sum \tag{1.0}$$

where Δu_i is dislocation, μ is the rigidity, w^k_{ij} are the displacement Green's functions due to a set of strain nuclei and n_j are the direction cosines of the normal to the surface element $d\Sigma$. Analytical expressions of the displacement in the form of elevation changes Δh and gravity changes Δg are summarized by Okada, (1985) and Okubo, (1992), respectively.

(i) Explicit form for Elevation Changes (Δh) :

$$\Delta h(x_1, x_2) = \frac{1}{2\pi}(U_1 S_h(\xi,\eta) + U_2 D_h(\xi,\eta) + U_3 T_h(\xi,\eta)) \;|\;| \tag{2.0}$$

where

$$S_h(\xi,\eta) = -\left[\frac{dq}{R(R+\eta)} + \frac{q\sin\delta}{R+\eta} + I_4\sin\delta\right],$$

$$D_h(\xi,\eta) = -\left[\frac{dq}{R(R+\xi)} + \sin\delta\tan^{-1}\left(\frac{\xi\eta}{qR}\right) - I_5\sin\delta\cos\delta\right] \tag{3.0}$$

S_h and D_h are the strike-slip and dip-slip component that caused elevation changes.
where

$$I_4(\xi,\eta) = (1-2\nu)\sec\delta[\log(r+d) - \sin\delta\,\log(R+\eta)]$$
$$I_5(\xi,\eta) = 2(1-2\nu)I_1\sec\delta$$
$$I_1(\xi,\eta) = \tan^{-1}\left(\frac{-q\cos\delta + (1+\sin\delta)(R+\eta)}{\xi\cos\delta}\right) \qquad (4.0)$$
$$R = \sqrt{\xi^2+\eta^2+q^2}$$
$$q = x_2\sin\delta - (d-x_3)\cos\delta$$
$$d = \eta\sin\delta - q\cos\delta$$

$|\,|$ denotes the double vertical introduced by Chinnery, (1961)

$$f(x, h)\,|\,| = f(x_1, p) - f(x_1, p\text{-}W) - f(x_1\text{ -}L, p) + f(x_1, \text{-}L, p - W) \qquad (5.0)$$

where $p \equiv x_2\cos\delta + (d - x_3)\sin\delta$

(ii) Contribution of dilatation field to gravity change Δg^*

$$\Delta g^*(x_1,x_2) = \{\rho G[U_1 S_g^*(\xi,\eta) + U_2 D_g^*(\xi,\eta) + U_3 T_g^*(\xi,\eta) + \Delta\rho G U_3 C_g^*(\xi,\eta) \quad |\,| \qquad (6.0)$$

where S*g and D*g are strike-slip and dip-slip components contribute to gravity change from the dilatation field, and is given by:

$$S_g^*(\xi,\eta) = I_4\sin\delta$$
$$D_g^*(\xi,\eta) = -I_5\sin\delta\cos\delta \qquad (7.0)$$

In this study, the accumulated gravity anomaly will be computed using formula of gravity changes Δg^* free from the effect of uplift or subsidence because we are to compare the result with data after removing terrain effect.

4. GRAVITY DATA - REDUCTION AND FILTERING PROCEDURES

New gravity stations have been established by using a model G-LaCoste & Romberg gravimeters over the test area, and their distributions is shown in Figure 4. Nearly 70% of measurements were carried out at points with spot height shown on 1:25000 scale topographical maps of Geological Survey Institute of Japan. Horizontal coordinate of each station was determined on a map using digitizer maintaining accuracy of 0.01'. Coordinates of the remaining 30% of the gravity points were determined by fast static GPS to realize homogeneous distribution of gravity stations with spacing approximately 500m around the fault area. Gravity measurements were performed using the closed loop method. A bench mark GSI BM586 at Chino City (where g = 979612.91 mgal, H = 788.10m) was adopted as a base station. Misclosure was kept below 50 microgal, which arose from non-linearity of instrumental drift and possible tares of the

gravimeters. Elapsed time of each loop was 6 to 8 hours. Observed data were reduced correcting earth tide and the instrumental drift on the daily basis. Details of gravity measurements and reduction procedures for the test area are fully discussed in Alias, (1995).

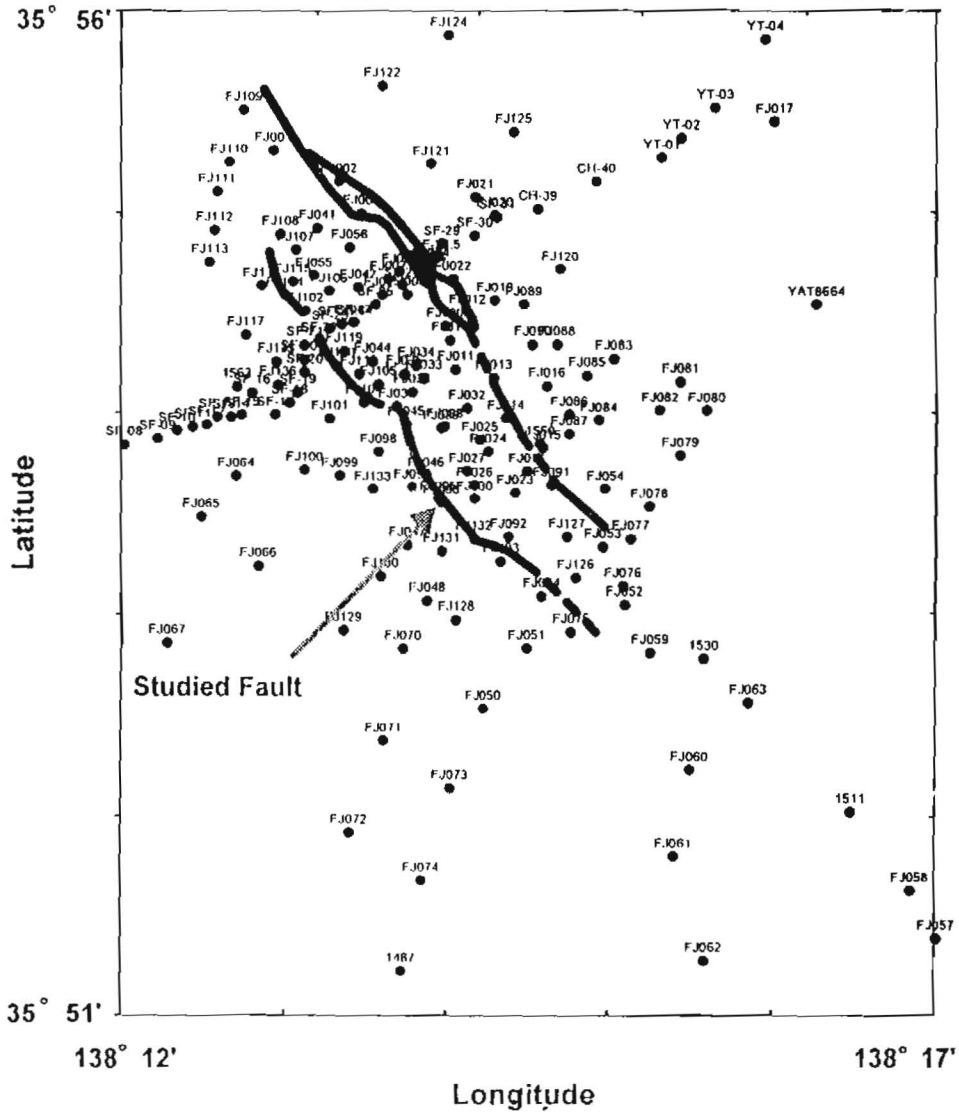

Figure 4 - The Distribution of Gravity Points in the Test Area

The errors of the gravity values at each point arise from two sources:

(a) Errors of the reference gravity at base (< 0.05 mgal in JGSN75 system), and

(b) The measuring errors of the relative gravity (<0.05 mgal).

In total the accuracy of the absolute gravity at each point is thus estimated to be better than ±0.1 mgal.

In order to create the 'detrended anomalies', we carried out the reduction and filtering procedures that is to remove the local gravity effect of the studied fault area.

A Bouguer anomaly value Δg_B is evaluated from a measured gravity value g_o through the reduction formula:

$$\Delta g_B = g_o - \gamma - \beta H + 2\pi G\rho H + TC \qquad (8.0)$$

where H is the orthometric height; γ is the normal gravity defined in International Gravity Formula 1980; and TC is the spherical terrain correction. The vertical gradient gravity β was assumed to be 0.3086 mgal/m .

The spherical terrain correction was computed using digital terrain model (DTM) KS 110-1 supplied by GSI; grid spacing 8."5 (latitude) x 11."25 (longitude) In the gravity reduction, the mean density ρ is adopted as 2.5 g/cm^3.

A filtering process has been applied to the raw gravity anomaly for extracting the effect of the fault motion on local gravity. The filtering process is very useful for detecting and locating weak anomalies against strong regional background. The filtering procedure was undertaken as follows:

(i) Preparation of two datasets, one including all the gravity data and the other excluding data around a window of (4km x 1km) of the studied fault.

(ii) The interpolation of gridded datasets using Kriging method, denoted as g_{all} and g_{window}. g_{window} represents regional gravity anomaly free from the local effect due to considering fault.

(iii) The subtraction of g_{window} from g_{all} to estimate the effect of faulting (g_{fault}). The output of the filtering process, i.e. g_{fault} is called detrended gravity anomaly because regional gravity trend is removed.

5. MODELLING AND RESULTS

As mentioned in section 3.0, the computation gravity changes and the expected coseismic elevation (topography) needs parameters such as the fault location, length L and width W of the fault, dip angle δ and dislocation magnitudes U. In this study, we computed the gravity changes due to fault motions on a rectangular plane in a homogeneous half-space. The flowchart of the measurements and modelling procedures is illustrated in Figure 5. From this modelling procedure, if the computed gravity anomaly and topography are in good agreement with the actual data (observations), then it can be said that the Accumulation Hypothesis has passed the test.

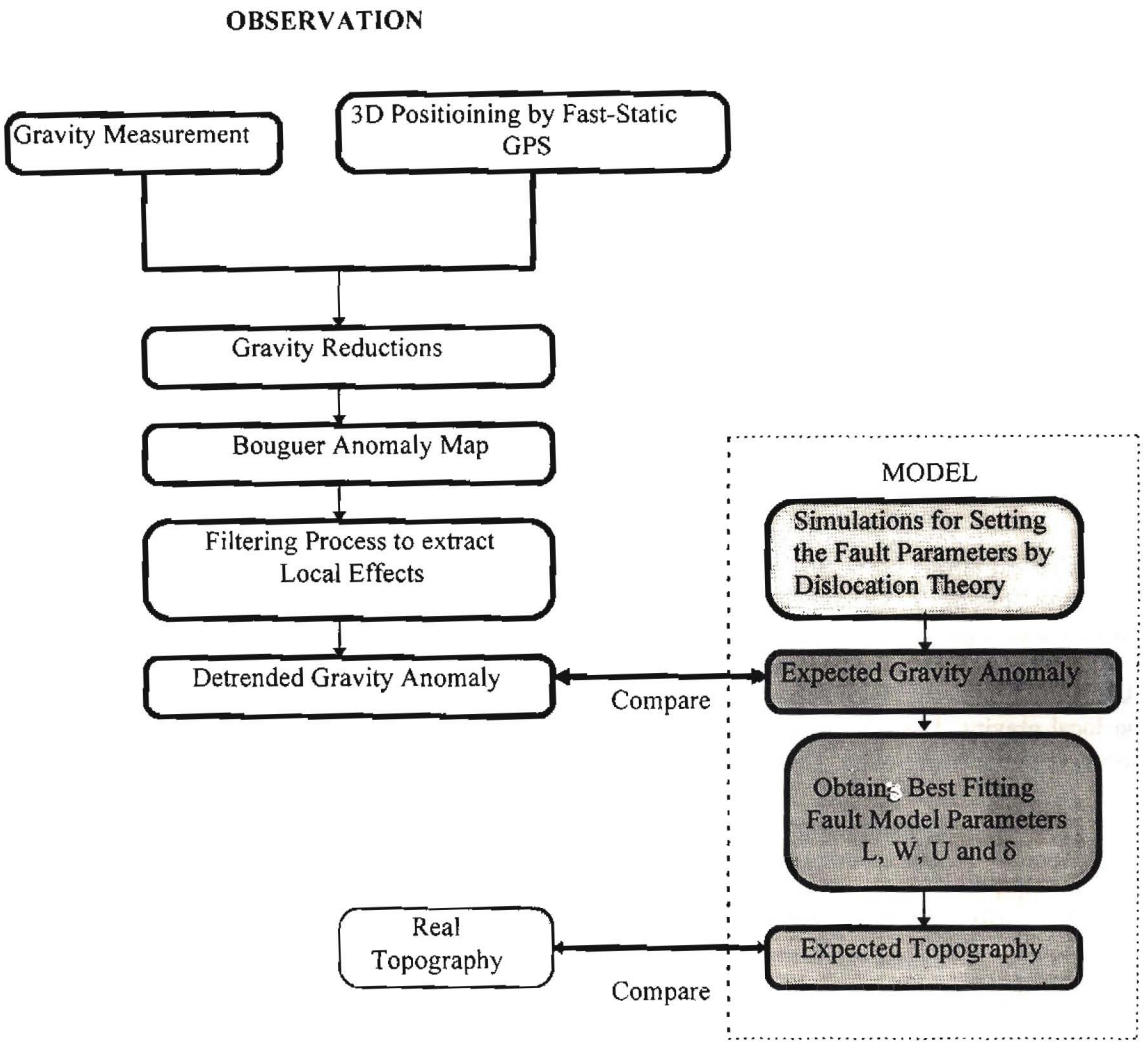

Figure 5 - The Flowchart of the Working Procedures

In general,the fault dimension parameters (L x W) determine the location and spatial extent of the gravity anomaly and topography. Meanwhile minimum and maximum values are dictated by the magnitude of dislocation (U_1 and U_2). We run the simulation process (trial and error) to obtain the fault parameters (L, W, U and δ) which reasonably explained the observed gravity data. These favoured dislocation parameters is shown in Table:-1.0.

L	Length	2 km
W	Width	3 km
D	Depth to top	0
U_1	Strike slip component	100 m
U_2	Dip slip component	-50 m
δ	Dip angle	80°

Table 1.0 - The Favoured Parameters for the Chosen Fault

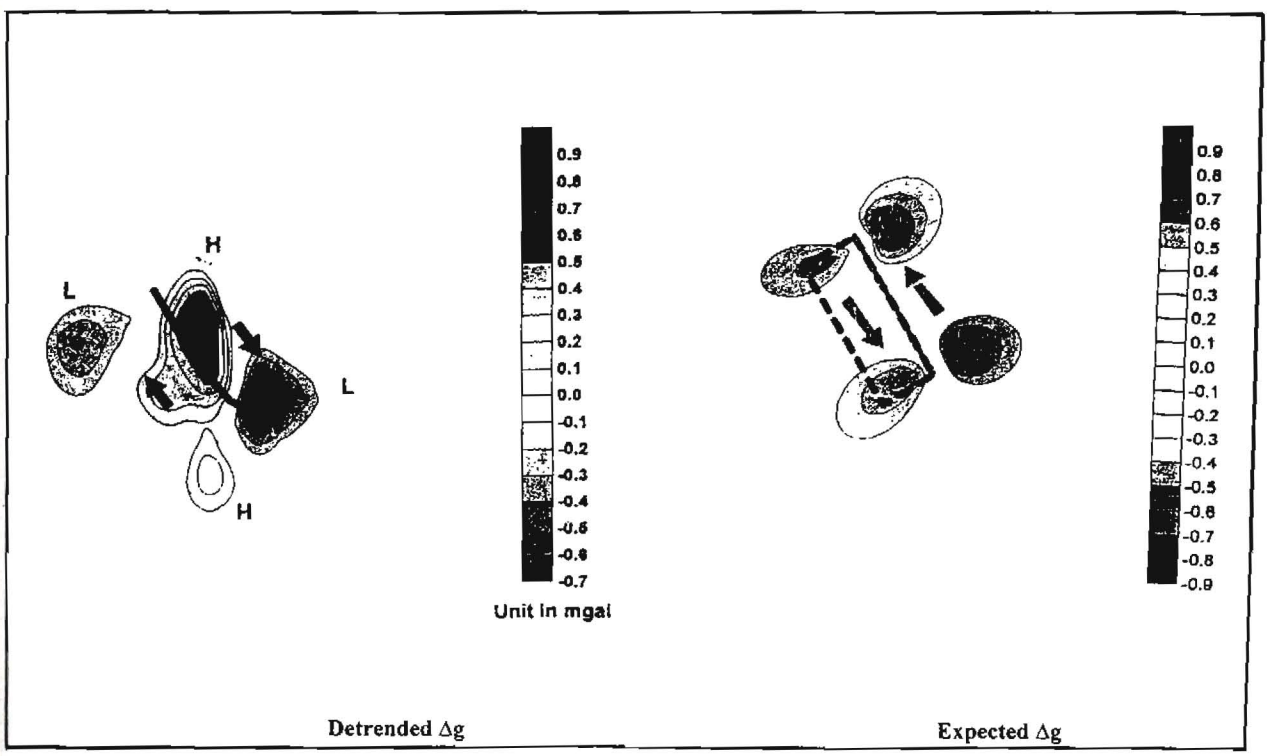

Figure 6 - Comparison Between Observed and Expected (Model) Data

The expected gravity anomaly is shown in Figure: 6. From the above figure, it can be seen that the characteristic quadrant pattern of gravity anomaly was estimated between - 0.7 to 1.0 mgal that suggests predominant strike-slip faulting. These estimated gravity anomalies agreed well to that of the detrended gravity anomaly , both in magnitude and locations of local minimum and maximum. However, the expected maximum uplift turns out to be only 22 meters, slightly lower than the real topography (estimated about 30 to 40 meters high). Based on the above favoured paramaters, the elevation changes are estimated and compared with the actual topography of the fault area. Figure: 7 and Figure: 8 show the estimated and the actual topography of the fault area, respectively.

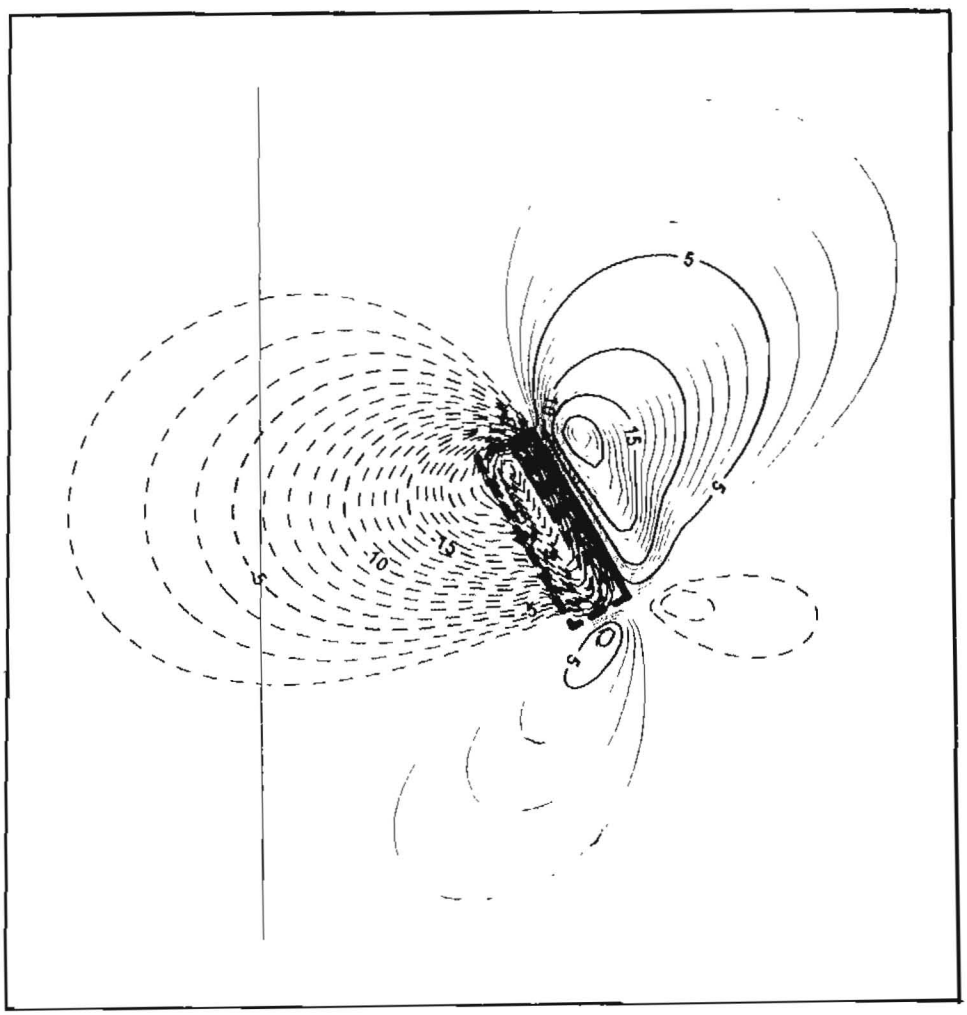

Figure 7 - The Expected Topography of the Fault Area

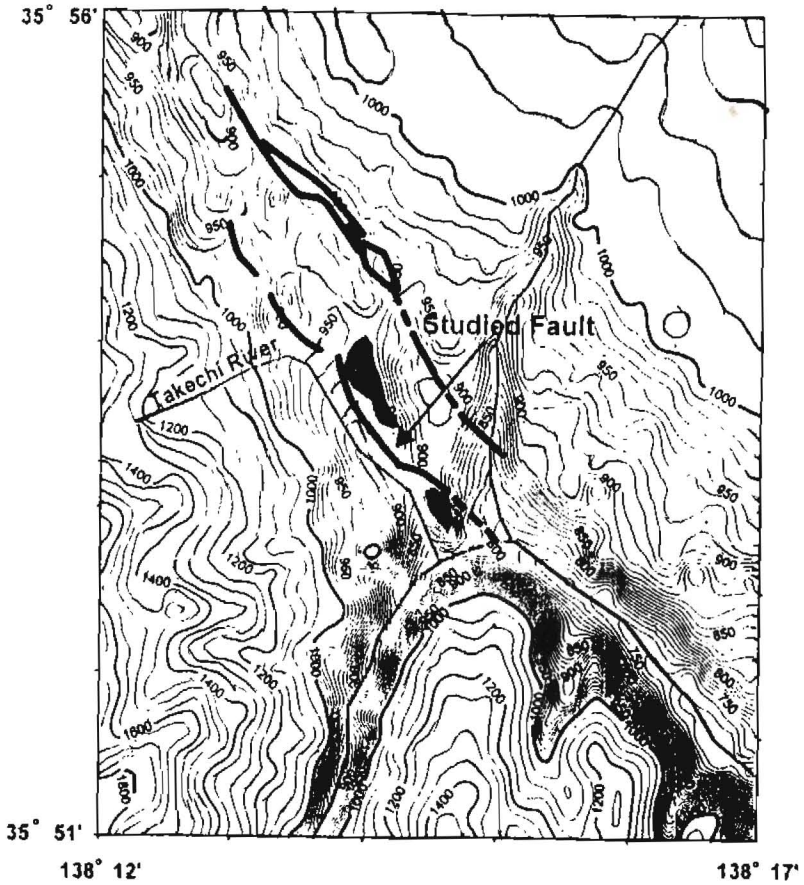

Figure 8 - The Actual Topography of the Fault Area

Figure: 7 shows that the elevation changes were estimated between -31m to 22m. The solid lines represent uplift while the broken lines indicate subsidence. From the same figure, it is shown that the expected topography has a fairly good agreement with the actual topography of the fault area (Figure: 8). The estimated topography, however, exhibits the two tectonic bulges in a quadrant pattern. Here, it is believed that the repeated earthquakes have generated the tectonic bulges in the uplift area by pulling up coseismic uplift in a systematic may. However, the sag ponds are not found in the subsidence area. This is well explained by geomorphological process such as sedimentation because Takechi river runs besides the studied fault line depositing soils in a fan-shaped manner.

6. CONCLUSION

Local gravity anomaly around the active fault reflects past activities of the fault. In particular, we find that a simple fault model yields gravity anomaly in a quadrant pattern which agreed well with the observations (detrended gravity). The same model also generates elevation changes that is consistent with the actual topography of the fault area. Moreover, the detrended gravity anomaly and geomorphology showed the occurance of a strike-slip and a dip-slip fault motions. Finally, as expected from the Accumulation Hypothesis, we found that the lower and higher gravity anomaly is exhibited in dilated and compressed areas, respectively.

Acknowledgement:
We would like to express many thanks to Prof. Dr.I. Murata and Dr. Okubo, S. for their supplying the relevent data and materials towards this study.

REFERENCES

Chinney, M.A., (1961) : *The deformation of ground surface fault.* Bull. Seis. Soc. Am., 51.
Harigawa, Y., (1967) : *Analyses of Gravity Values in Japan.* Bull. Earthq. Res.Inst. Univ. Tokyo 45.
Ilias, S., (1995) : *Gravity Anomaly and Topography Induced by Repeated Fault Motions.* Unpublished M.Sc Dissertation. Earthquake Research Institute, The University of Tokyo, Japan.
Okada, Y., (1985) : *Surface Deformation due to Shear and Tensile Faults in a Half-space,* Bull Seis. Soc. Am., 75, 1018-1040.
Okubo, S., (1989) : *Gravity Changes Caused by Fault Motion on Finite Rectangular Plane.* J. Geod. Soc. Jpn., 35, 159-164 .
Okubo, S., (1992): *Gravity and Potential Changes due to Shear and Tensile in a Half-space,* J. Geophys. Res, 97, B5, p. 7137 - 7144.